Journal Pre-proof

Thermo-catalytic co-pyrolysis of palm kernel shell and plastic waste mixtures using bifunctional HZSM-5/limestone catalyst: Kinetic and thermodynamic insights

April Ling Kwang Chee, Bridgid Lai Fui Chin, Sharon Meng Xuang Goh, Yee Ho Chai, Adrian Chun Minh Loy, Kin Wai Cheah, Chung Loong Yiin, Serene Sow Mun Lock

PII: S1743-9671(23)00023-5

DOI: https://doi.org/10.1016/j.joei.2023.101194

Reference: JOEI 101194

To appear in: *Journal of the Energy Institute*

Received Date: 3 January 2023

Revised Date: 25 January 2023

Accepted Date: 30 January 2023

Please cite this article as: A.L.K. Chee, B.L.F. Chin, S.M.X. Goh, Y.H. Chai, A.C.M. Loy, K.W. Cheah, C.L. Yiin, S.S.M. Lock, Thermo-catalytic co-pyrolysis of palm kernel shell and plastic waste mixtures using bifunctional HZSM-5/limestone catalyst: Kinetic and thermodynamic insights, *Journal of the Energy Institute* (2023), doi: https://doi.org/10.1016/j.joei.2023.101194.

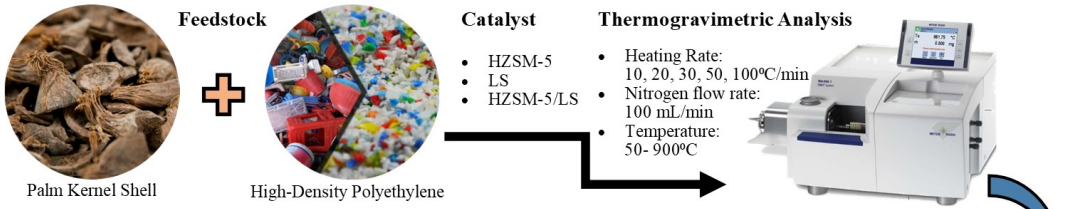

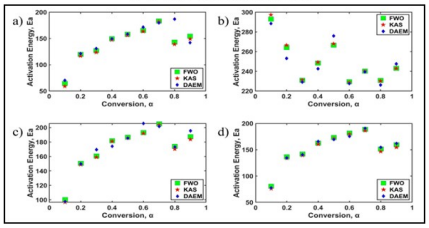

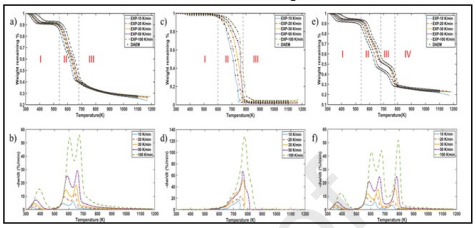

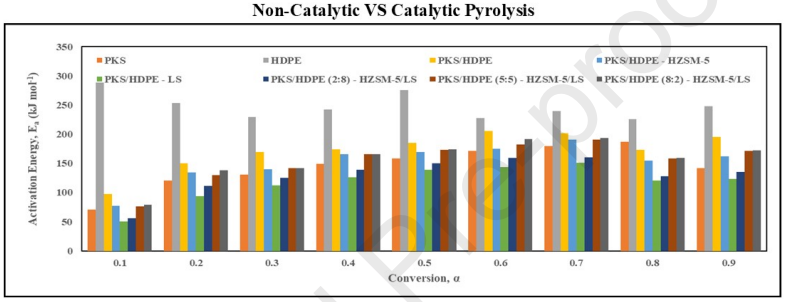

Thermo-catalytic Co-Pyrolysis of Palm Kernel Shell and Plastic Waste Mixtures using Bifunctional HZSM-5/Limestone Catalyst: Kinetic and Thermodynamic Insights

April Ling Kwang Chee[a], Bridgid Lai Fui Chin[a,*], Sharon Meng Xuang Goh[a], Yee Ho Chai[b], Adrian Chun Minh Loy[c] , Kin Wai Cheah[d] , Chung Loong Yiin[e] , Serene Sow Mun Lock[f]

[a]Department of Chemical and Energy Engineering, Faculty of Engineering and Science, Curtin University Malaysia, CDT 250, 98009 Miri, Sarawak Malaysia.

E-mail: (1) 700029897@student.curtin.edu.my (April Ling Kwang Chee)

(2) bridgidchin@gmail.com; bridgidchin@curtin.edu.my (Dr Bridgid Lai Fui Chin)*

(3) 700031739@student.curtin.edu.my (Sharon Meng Xuang Goh)

*Corresponding author

[b]HiCoE - Centre for Biofuel and Biochemical Research, Institute of Self-Sustainable Building, Universiti Teknologi PETRONAS, Seri Iskandar, Perak 32610, Malaysia.

E-mail: yeeho.chai@utp.edu.my

[c]Department of Chemical Engineering, Monash University, Clayton VIC 3800, Australia.

E-mail: adrian.loy@monash.edu

[d]School of Computing, Engineering and Digital Technologies, Teesside University, Middlesbrough TS1 3BX, United Kingdom.

E-mail: k.cheah@tees.ac.uk

[e]Department of Chemical Engineering and Energy Sustainability, Faculty of Engineering, Universiti Malaysia Sarawak (UNIMAS), Kota Samarahan 94300, Sarawak, Malaysia.

E-mail: clyiin@unimas.my

[f]CO_2 Research Center (CO2RES), Department of Chemical Engineering, Universiti Teknologi PETRONAS, 32610 Seri Iskandar, Malaysia

E-mail: sowmun.lock@utp.edu.my

Abstract

Kinetic and thermodynamic parameters of catalytic co-pyrolysis of palm kernel shell (PKS) and high-density polyethylene (HDPE) with three different catalysts (zeolite HZSM-5, limestone (LS) and bifunctional HZSM-5/LS) using thermogravimetric

analyser via nitrogen environment were studied. The experiments were carried out at different heating rates ranging from 10 to 100 K min^{-1} within temperature range of 50-900ºC. Flynn-Wall-Ozawa (FWO), Kissinger-Akahira-Sunose (KAS) and modified Distributed Activation Energy Model (DAEM) methods were employed in this current study. The average E_a for PKS, HDPE, PKS/HDPE (2:8) – HZSM-5, PKS/HDPE (2:8) – LS, PKS/HDPE (2:8) – HZSM-5/LS, PKS/HDPE (5:5) – HZSM-5/LS, PKS/HDPE (8:2) – HZSM-5/LS are 137.26-145.49, 247.73-250.45, 168.97-172.50, 149.74-152.79, 115.30-120.39, 124.36-129.41, 151.03-154.47 and 152.67-157.31 kJ mol^{-1}, respectively. Among the different catalysts used, LS demonstrated the lowest average E_a (151.30-120.39 kJ/mol) and ΔH (109.65-114.74 kJ mol^{-1}). Positive values for ΔH and ΔG were found for the catalytic co-pyrolysis of PKS/HDPE mixtures which indicates the process is in endothermic reaction and possess non-spontaneous nature. The kinetic and thermodynamic analyses revealed the potential of PKS and HDPE as a potential feedstock for clean bioenergy production.

Keywords: Co-pyrolysis; Palm Kernel Shell; High-Density Polyethylene; Kinetic; Thermodynamic; Catalytic.

1.0 Introduction

As the world population increases, the demand for resources surges exponentially over the years as a result of extensive human activities to accommodate for the growing population. This exerts a downward pressure on the resources available. Non-renewable resources, particularly the fossil fuels, which have been on the brink of extinction have ignited the exploration of energy resources with greater sustainability and are environmentally friendly. In fact, fossil fuels have been the major source towards primary energy consumption. This can be evidenced through the upsurge of consumption demand

for fossil fuels by approximately 51% between 1995 and 2015 and the percentage was believed to be further increasing by at least 18% by 2035 [1]. The subsequent effect of huge dependence on fossil fuels is the intense change of global climate and environmental deterioration due to greenhouse gases (GHGs) effect. These have been major global concerns that gained the public attention and therefore drives the energy system paradigm shift of fossil fuels to renewable energy sources.

One of the potential alternatives to alleviate the dependence on conventional fuels would be the utilization of biomass. The carbon neutral nature of biomass makes it a valuable clean alternative renewable energy resource which could be contributing to a substantial share of the world's primary energy mix as an effort to mitigate global warming and promote sustainability. Palm kernel shell (PKS) is deemed to be a potential biomass energy source due to its abundant production by palm oil mills. PKS also consist of relatively high carbon content and fixed carbon content of 51 wt% and 34 wt% respectively [2]. The benefits of high carbon content include producing biochar with greater resistance and stability [3]. Based on the statistics released by Malaysia Palm Oil Board (MPOB), the total amount of crude palm oil of 3.4 million tonnes produced a corresponding amount of palm oil waste of 25.5 million tonnes in 2016 [4]. In the following year 2017, a total amount of 2.1 million tonnes of crude palm oil was produced while a total of 80 million tonnes of biomass was generated [4]. The statistics show that lower amount of crude oil was produced yet the palm oil biomass was increased by a factor of 3 is a concerning issue as massive amount of waste could result in serious environmental degradation if the wastes are not properly treated or disposed of. The subsequent event of this is the sparked interest of researchers to delve into the utilisation of palm oil wastes as a biomass feedstock for generating bioenergy [5-6].

The invention of plastics has certainly brought up a new world of possibilities and has since then bring forth the greatest convenience upon the human population. Despite its contribution to the raising of living standards to the humankind, the continuous demand of plastics has also led to the rising amount of waste produced. Consequently, more spaces would be consumed which also leads to environmental issues such as polluted environments which affects the ecosystem. It was reported that the global plastic output has exceeded 8.3 BNt [7], with yearly production close to 360 Mt, and the annual production is anticipated to double in 20 years as a result of the high consumer demand [8]. The tremendous growth of plastic wastes due to poor management has brought huge concerns to the public. As a result, alternative ways to manage and reuse these plastic wastes have been developed as an attempt to reduce their impact on the environment. One of the most prevailing ways to deal with the plastic waste is recycling. However, the recycling process itself is costly and has rather strict requirements in terms of separation of wastes. Another waste management approach would be utilizing plastic waste for energy recovery which makes plastic a useful renewable feedstock. One of the potential methods for this energy recovery is pyrolysis which is meant to thermally break down long chain of polymer molecules into simpler and smaller molecules.

Pyrolysis is one of the thermochemical biomass conversion methods that produces biofuels by burning biomass under very high temperatures in an oxygen-deficient environment. Pyrolysis has gained its prominence due to the benefits it brings along in terms of bioenergy production. Pyrolysis possesses carbon negative property and produces bio-oil, biogas and biochar that are able to meet the circular economy and hydrocarbons closed-loop recycling process [9]. It was found that pyrolysis based models produced greater overall process efficiencies and had the capability to promote greener

economy through significant contributions towards environmental mitigation [10]. Besides that, pyrolysis also has the capability of alleviating a country's reliance on imported energy resources as it allows energy to be generated from domestic resources and therefore facilitating the management of wastes especially in developing countries. For example, Malaysia government had established the National Green Technology Policy 2009 to intensify the renewable energy share in power generation and implementation of the green products for different applications. These steps were taken in order to attain effective renewable energy generation [11]. The need of using renewable energy for electricity generation was again re-emphasized in a new energy policy created under the Tenth Malaysia Plan (2011-2015) [12]. The main goal of this present study is to update knowledge on strategies for converting biomass and plastic waste in achieving Sustainable Development Goals (SDG) 7 i.e. affordable and clean energy in a sustainable manner. In keeping with commitment to the SDGs and Paris Agreement on climate change, the successful commercialization of this technology would have a significant impact on decarbonization efforts.

Several in-depth reviews have documented on the pyrolysis of plastic wastes, and lignocellulosic biomass. Hassan et al. [13] had performed a review specifically on the catalytic co-pyrolysis of biomass, plastic and coal mixtures. It is found that the presence of acid catalyst can enhance both the yield and selectivity of the products [13]. Ma et al. [14] had conducted a critical review on the mechanism involved in the co-pyrolysis process of biomass and plastic waste mixtures. Hassan et al. [15] mentioned that high density polyethylene (HDPE) can be used as a hydrogen-supplement for co-pyrolysis of biomass and possibly brings forth improvements to the quality of the biofuel in terms of calorific value and heating value.

Catalyst-driven pyrolysis is believed to bring forth enhancement purposes on not only the yields of the pyrolytic products but also their quality and selectivity. This is proven in the study conducted by Zhang et al. [16] where the application of zeolites catalyst on the pyrolysis of lignin had significantly improved the yields of pyrolytic liquid, selectivity to aromatic hydrocarbons and product quality. Based on their study, it was deduced that desirable products are attainable through the translation of depolymerized intermediates by catalysts. Meanwhile, the catalysts also functioned as an inhibitor to prevent repolymerization and therefore reduce the char formation [16]. Research results obtained by Tan et al. [17] have shown that zeolite HZSM-5 catalyst is the most effective catalyst for the pyrolysis of biomass when considering the product yields and reduction in coke formation. Besides that, catalysts also play a substantial role in the reduction of activation energy of a process for economic reasons as low activation energy implies less energy requirement for the initiation of a process and therefore low cost may be needed. There are several studies found in literatures utilising zeolite HZSM-5 [18-19], natural limestone (LS) [18,20], and bifunctional HZSM-5/LS as catalysts in pyrolysis process [18]. However, to the best of the author's knowledge, the recent investigation on the co-pyrolysis of the palm kernel shell (PKS) and plastic waste mixtures with the presence of commercial zeolite HZSM-5, LS, and bifunctional HZSM-5/LS had not been investigated.

Therefore, this study aimed at investigating the thermal degradation, kinetic and thermodynamic analysis of the catalytic co-pyrolysis of PKS and high-density polyethylene (HDPE) mixtures behaviour via thermogravimetric analysis (TGA) approach. This study incorporates the use of zeolite H-ZSM5, LS, and H-ZSM5/LS as the catalyst to enhance the conversion of the feedstock for bioenergy production. Modified DAEM and iso-conversional methods such as Flynn-Wall-Ozawa (FWO), and Kissinger-

Akahira-Sunose (KAS) are the kinetic modelling approaches for determining the kinetic parameters such as activation energy (E_a), pre-exponential (A). The DAEM model itself has been a successful approach for biomass pyrolysis due to its accountability for kinetics of complex reactions whereby pyrolysis is assumed to be constituted of parallel first order reactions [21]. The FWO method is the most popular used iso-conversional method which can be used without assuming the order of reaction and applied in a broad range of degree of conversion [22]. Meanwhile, KAS method is said to have a higher accuracy compared to FWO method [22]. Furthermore, the thermodynamic parameters such as enthalpy change (ΔH), Gibb's free energy (ΔG), and entropy change (ΔS) will also be evaluated using the FWO and KAS methods. Results obtained from the modified DAEM and iso-conversional methods will be compared to verify the accuracy and reliability of these models in determining the kinetic parameters in the study of the catalytic co-pyrolysis of PKS and HDPE. And also, our research has revealed several key mechanistic aspects of catalytic co-pyrolysis of plastic and biomass waste mixtures. There are few studies found in literatures focused on both kinetic and thermodynamic analyses particularly for pyrolysis process are found in [23-25].

2.0 Materials and methods

2.1 Feedstock characterization

The PKS was obtained from the local palm-oil mill in Miri, Malaysia whereas the HDPE was attained from Shen Foong Trading Sdn. Bhd., Tronoh Malaysia. For the plastic HDPE's proximate analysis, it comprised of (0.34±0.11)% ash content, and (99.46±0.21)% volatile matter. Meanwhile, the biomass PKS was consisted of (66.90±0.10)% volatile matter, (7.90±0.20)% moisture content, (22.6±0.22)% fixed carbon, and (2.6±0.13)% ash. Based on the dry basis for the HDPE, the ultimate analysis of carbon, hydrogen, nitrogen,

sulphur, and oxygen contents were 81.45 wt%, 12.06 wt%, 0.34 wt%, 0.79 wt%, and 5.46 wt%, respectively. Based on the dry basis for the PKS, the ultimate analysis of carbon, hydrogen, nitrogen, sulphur, and oxygen contents were 54.72 wt%, 7.2 wt%, 0.42 wt%, 0.26 wt%, and 37.4 wt%, respectively.

All the catalyst preparation and experimental procedures can be found in the **supplementary material.**

2.2 Kinetic Theory

Pyrolysis of solid biomass can be considered as a single-step global process, assuming that the solid biomass is converted into volatiles and char at a rate constant *k* as defined by Eq. (1).

$$Solid \xrightarrow{k} Volatiles + Char \quad (1)$$

The graphical results from the TGA experiments conveys the thermal degradation behaviour of the PKS and HDPE feedstock, whereby the kinetic parameters such as activation energy and pre-exponential factor can be determined.

Following the theory of reaction kinetics, the expression of solid-state devolatilization for non-isothermal conditions is as shown in Eq. 2.

$$\frac{d\alpha}{dt} = k(T)f(\alpha) \quad (2)$$

$$g(\alpha) = k(T)t \quad (3)$$

where α is the degree of conversion, $\frac{d\alpha}{dt}$ is the rate of reaction, $k(T)$ is the reaction rate constant, $f(\alpha)$ is the differential reaction model, $g(\alpha)$ is the integral reaction model and t is the reaction time.

Assuming first order reaction takes place, it can be defined as shown in Eq. 4.

$$\frac{d\alpha}{dt} = k(1-\alpha) \quad (4)$$

Meanwhile, for n^{th} order reaction, it is defined in Eq. 5.

$$f(\alpha) = (1-\alpha)^n \quad (5)$$

The degree of conversion (α) can be expressed as Eq. 6 which is defined in terms of weight difference upon undergoing TGA.

$$\alpha = \frac{m_0 - m_t}{m_0 - m_f} \quad (6)$$

where m_0 is the initial weight (mg), m_t is the instantaneous weight at time 't' and m_f is the final weight after pyrolysis.

The k variable can be described by the Arrhenius equation as shown in Eq. 7.

$$k(T) = Ae^{-\frac{E_a}{RT}} \quad (7)$$

Where k is the reaction rate constant, α is the degree of conversion, A is the pre-exponential factor (s^{-1}), E_a is the activation energy (kJ/mol), R is the universal gas constant (8.314 J/(mol·K)) and T is the absolute temperature (K).

Substitute Eq. 5 into Eq(s) 1 and 2 to obtain Eq(s) 8 and 9.

$$\frac{d\alpha}{dt} = Ae^{-\frac{E_a}{RT}} f(\alpha) \quad (8)$$

$$g(\alpha) = Ae^{-\frac{E_a}{RT}} t \quad (9)$$

Assuming non-isothermal conditions with a constant heating rate β, $\beta = \frac{dT}{dt}$, Eq(s) 10 and 11 are obtained by substituting $\beta = \frac{dT}{dt}$ into Eq(s) 7 and 8.

$$\beta \frac{d\alpha}{dT} = Ae^{-\frac{E_a}{RT}} f(\alpha) \quad (10)$$

$$g(\alpha) = \int_0^{\alpha} \frac{d\alpha}{f(\alpha)} = \frac{A}{\beta} \int_{T_0}^{T} e^{-\frac{E_a}{RT}} dT \quad (11)$$

Eq(s) 10 and 11 are used for the determination of the kinetic parameters based on the TGA experimental data, using modified DAEM model and iso-conversional methods which are the FWO and KAS (**see supplementary materials**).

2.3 Thermodynamic Analysis

The E_a obtained from the kinetic modelling would be used to determine the thermodynamic parameters such as enthalpy change, entropy change and free Gibb's energy. These parameters can be calculated by Eq(s) 12-14.

$$\Delta H = E_a - RT_\alpha \quad (12)$$

$$\Delta G = E_a + RT_m \ln\left(\frac{K_B T_m}{hA}\right) \quad (13)$$

$$\Delta S = \frac{\Delta H - \Delta G}{T_m} \quad (14)$$

where K_B is the Boltzmann constant ($1.381 \times 10^{-23}\, J \cdot K^{-1}$), h is the Plank constant ($6.626 \times 10^{-34}\, J \cdot S$), T_m is the derivative thermogravimetric (DTG) peak temperature and T_α is the temperature at the degree of conversion (α).

3.0 Results and Discussion

3.1 Thermal Degradation Behaviour

3.1.1 Palm Kernel Shell (PKS)

The thermogravimetric (TG) and derivative thermogravimetric (DTG) curves show that heating rates plays a significant role in the thermal degradation as the curves shift towards the higher temperatures with greater mass loss rate when the heating rate is increased.

Similar behaviour and trends of thermal degradation have also been attained by a few studies whereby the authors have ascertained that the heating rates indeed influences the maximum rate of thermal degradation [26–29]. It was suggested that high heating rate tend to result in greater rate of maximum decomposition as more heat energy allows enhanced heat transfer between the insides of the samples and the surroundings [26].

The pyrolysis process of PKS comprises of three main stages of decomposition. The primary thermal decomposition, which is the first stage of pyrolysis (Stage I), is where the moisture content is vaporized. Referring to Fig. 1(a), Stage I takes place around temperature between 300K and 550K. The temperature range of Stage I is slightly greater than that of the results obtained by Surahmanto et al. [26] which was between 300 K and 493 K. This could be due to the different level of moisture content in the PKS samples and thereby resulting in slightly different temperature range for vaporization of moisture. Higher moisture content in the PKS sample of this study may have caused the greater range of temperature for vaporization to take place.

The second stage (Stage II) corresponds to the devolatilization of hemicellulose and cellulose. The temperatures of Stage II extend over a rather short range which lies between 550 K and 700 K. Within the same temperature range, maximum mass losses with multiple peaks as demonstrated by the DTG curves are observed at different heating rates as shown in Fig. 1(a). Similar occurrence is also observed in the work by Surahmanto et al. [26]. Again, their temperature range for devolatilization is slightly lower than the results obtained in this study. In this case, the difference is attributable to the composition of cellulose and hemicellulose in the PKS samples. Since the PKS sample used in this study has greater proportions of cellulose and hemicellulose, the degradation temperature required would therefore be higher.

Subsequent to devolatilization is the char pyrolysis which is the third stage of decomposition (Stage III). Stage III takes place starting from temperature of about 700 K until it reaches the maximum operating temperature which is almost 1200 K. The third stage is mainly characterised by the prolonged 'tailing' of the curves with much gentle decreasing slopes. This stage is also ascribed to lignin decomposition.

In reference to Fig. 1 (b), smaller mass loss can be observed in Stage I with maximum mass loss rates of 15.29, 7.20, 4.51, 3.05 and 1.74 %/min at temperatures of 393, 370, 360, 352 and 342 K, respectively. During Stage II, the maximum loss rate further reached at a much higher rate and two main degradation peaks were observed. The maximum loss of mass is the most apparent at this stage. Consequently, the second stage could be deemed as the rate-determining step in the pyrolysis process. The first peak could be formed as a result of hemicellulose decomposition for which maximum mass loss rates are 53.63, 25.22, 14.67, 9.54 and 4.57 %/min at temperatures of 604, 589, 580, 572 and 560 K, respectively. The second peak would be linked to the cellulose decomposition whereby the maximum mass loss rates are 55.75, 29.07, 18.35, 12.55 and 6.43 %/min at temperatures of 672, 659, 650, 643 and 631 K, respectively.

3.1.2 High Density Polyethylene (HDPE)

Similar effect of heating rate on the pyrolysis of PKS is also observed in pyrolysis of HDPE. Lateral shifts of the TG and DTG curves to the right-hand side where the temperatures of the maximum degradation peaks are also shifted to a higher level can be observed when the heating rate is increased during the decomposition process. This implies that more reaction time was required for the minimum activation energy to be attained to allow the decomposition to occur. Furthermore, the TG and DTG curves have

284 also demonstrated an upward shift patten alongside with increasing heating rates which
285 indicates faster maximum degradation rate is achieved with the increment of heating rates.

286 The TG and DTG curves of HDPE has significant differences from those of the PKS due
287 to its components. Unlike PKS, HDPE does not have lignocellulosic components such as
288 cellulose, hemicellulose and lignin since it is a thermoplastic polymer. Therefore, HDPE
289 has only one peak in the DTG curves at each heating rate as the thermal decomposition
290 occurs in a single stage. Similar trend of results have also been observed in studies done
291 by others [27–36].

292 In reference to the TGA curve as represented by Figure 1 (d), the thermal degradation
293 began at the temperature of around 542K and extends until 746.53-859.34 K which
294 indicates completion of the pyrolysis process. In comparison with the pyrolysis of PKS
295 in which the thermal degradation spans over a wide range of lower temperatures, thermal
296 degradation of HDPE takes place at a significantly higher temperature. Ng et al. [33]
297 suggested that the characteristics of the material in terms of chemical structure and
298 composition as well as the heat source greatly affects the temperature of the thermal
299 degradation of the feedstock. Additionally, HDPE has more aromatic and aliphatic
300 character and thus exhibiting better thermal stability which implies the need for greater
301 temperatures for it to be decomposed [33].

302 As aforementioned, the DTG curves of HDPE consist of a single peak for each heating
303 rate. The maximum peak corresponds to the maximum degradation rate which increases
304 when heating rate is increased. The maximum rates of thermal degradation are observed
305 at temperatures of 740.22, 754.79, 769.44, 765.49 and 778.95K with rates of 18.03, 23.31,
306 52.03, 66.87 and 128.16 %/min, respectively.

3.1.3 Binary Mixture of PKS and HDPE with the Absence of Catalysts

The binary mixtures of PKS and HDPE in ratio of 2:8 have the TG and DTG curves are shown in Fig(s) 1(e) and 1(f) respectively. The selection of the PKS/HDPE mixture mass ratio was based on the optimum condition found in previous studies in literature of co-pyrolysis of biomass and plastic waste mixture [32]. Unlike the TG and DTG curves of the individual PKS and individual HDPE, the curves of the binary mixtures have a different trend of curves. Nevertheless, three stages of thermal degradation can still be observed from the curves as it tells the vaporization of moisture content and the decomposition of the lignocellulosic components in PKS. Stage I of the binary mixture, which corresponds to moisture vaporization, have begun at around 300 K and ends at about 550 K. This temperature range is identical to that of the individual PKS feedstock. Stage II, where decomposition of hemicellulose and cellulose occurs, then commenced thereafter and ends around 700 K which is again similar to that of the individual PKS feedstock. Stage II is trailed by Stage III, where HDPE degradation takes place, with the final temperature arriving at approximately 800 K. A dissimilar pattern can be observed in this stage in the TGA curve (Fig. 1(f)) which differs from that of the individual PKS feedstock. Since HDPE is also part of the mixture, its presence can be characterised by the curve between 690 and 805 K which corresponds to the decomposition of HDPE. In this case, the temperature range of the thermal degradation does not resemble that of the individual HDPE feedstock. This could be due to the synergistic effects existing between PKS and HDPE. This phenomenon is also observed in the works conducted by Chin et al. [32], Ng et al. [33], and Liew et al. [35]. It was suggested that the synergistic effect from the binary mixture of HDPE and rubber seed shell have led to an enhanced production of syngas [32]. Likewise, similar effect could be occurring for the binary mixture of HDPE

and PKS. The last stage, Stage IV, corresponds to the lignin decomposition as it is characterised by the trend of gentle slope extending over a wide range of temperature.

The DTG curve in Fig. 1(f) for the binary mixture shows the significant peaks that resembles that of the individual PKS and HDPE feedstock. However, the maximum degradation rates are generally lower than that of the individual feedstock. In Stage I, where vaporization of moisture content takes place, the maximum peaks which corresponds to maximum mass loss rates of 1.69, 2.62, 3,39, 5.56 and 11.97 %/min took place at 340, 355, 357, 367 and 388 K, respectively. In Stage II, the first peak, which represents the decomposition of hemicellulose, has maximum mass loss rates of 4.06, 8.60, 11.86, 20.90 and 43.06 %/min at temperatures of 562, 571, 580, 590 and 605 K, respectively. As for the second peak, where decomposition of cellulose takes place, the maximum mass loss rates are 5.81, 11.49, 15.06, 24.40 and 44.04 %/min for temperatures 631, 643, 651, 661 and 673 K, respectively. In Stage III, the peaks which represents the maximum mass loss rates for the HDPE occurred at temperatures of 751, 763, 772, 782 and 794 K with rates of 3.41, 6.41, 16.09, 24.79 and 51.63 %/min.

346

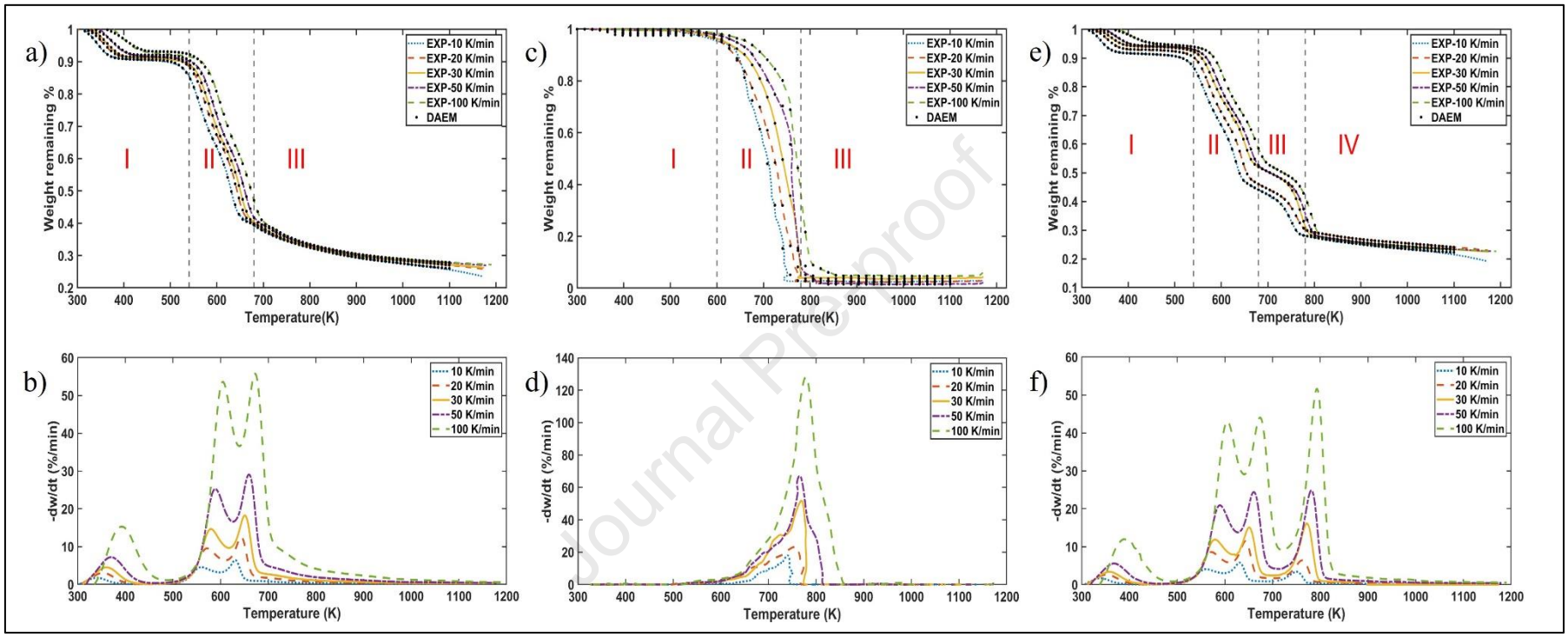

347

348 **Fig. 1.** (a) TG graph of non-catalytic pyrolysis of PKS, (b) DTG graph of non-catalytic pyrolysis of PKS, (c) TG graph of non-catalytic
349 pyrolysis of HDPE, (d) DTG graph of non-catalytic pyrolysis of HDPE, (e) TG graph of non-catalytic pyrolysis of binary mixture of
350 PKS/HDPE (2:8), and (f) DTG graph of non-catalytic pyrolysis of binary mixture of PKS/HDPE (2:8).

3.1.4 Binary Mixture of PKS and HDPE with the Presence of Catalysts

All TG curves of the catalytic pyrolysis of binary mixtures of PKS and HDPE, as illustrated by Fig(s) 2 (a)-(e), exhibit similar trends as that of the non-catalytic pyrolysis with the same range of temperatures observed for all stages, from Stage I to Stage III. This shows that consistent thermal degradation has taken place throughout the experiments for the binary mixtures. The mass blend ratios of PKS and HDPE mixture analysed with the presence of catalysts are in 2:8, 8:2, and 5:5, which are based on the optimum conditions found in previous studies of Aboulkas et al. [30] and Chin et al. [32].

The notable differences would be the maximum rate of mass loss at different heating rates, with different catalysts used, which are more evident in the DTG curves. For similar blend ratio of PKS and HDPE of 2:8, catalytic pyrolysis of binary mixtures of PKS and HDPE generally show lower mass loss rates than that of the non-catalytic pyrolysis. It is evident that the use of catalysts has the ability to reduce the loss of mass per unit time, especially for Stage II. The percentage reduction is at least 1.23% up to 43.52%. On the contrary, the presence of LS catalyst in the pyrolysis had resulted in a higher maximum mass loss rate in Stage I for heating rates 30, 50 and 100 K/min. Similarly, the presence of catalysts at lower heating rates of 10, 20, 30 K/min also resulted in greater maximum mass loss rates during Stage III. Catalyst with the best performance in lowering the maximum mass loss rate would be the bifunctional HZSM-5/LS catalyst which shows a maximum reduction of 43.52% for co-pyrolysis at 100 K/min during Stage III when compared to individual performance of HZSM-5 and LS. HZSM-5 catalyst is observed to show better performance at lower heating rates, generally at 10-20 K/min, during Stage I (moisture vaporization). This could be due to the enhanced conversion of lignocellulosic biomass into pyrolytic vapours which enters the zeolite catalysts active sites to form carbon

monoxide, carbon dioxide and water [37]. At higher heating rates, the catalytic effect of HZSM-5 catalyst is restricted by the presence of cellulose and lignin [38]. LS catalyst, on the other hand, shows better performance at higher heating rate of 30-50K/min during Stage I (moisture vaporization) and Stage II (decomposition of hemicellulose and cellulose). Study conducted by Chen et al. [39] have found that LS promoted the decarbonylation of ketones and formation of hydrocarbons during hemicellulose pyrolysis as well as boosted the ring-opening and dehydration reactions during the cellulose pyrolysis. For the same blend ratio of 2:8, HZSM-5 catalyst shows highest maximum degradation rates during Stage III (decomposition of HDPE). This is because HZSM-5 catalyst is able to reduce the thermal stability of HDPE through cracking reactions catalysed by the acid sites on the surface of the catalyst [38].

For the same bifunctional catalyst, taking blend ratio of 2:8 as the reference, blend ratio of 5:5 would generally give lower maximum mass loss rates than that of the ratio of 8:2. This suggest that as the proportion of PKS in the binary mixture increases, the maximum mass loss rate may decrease. However, this trend is only seen in Stage I (moisture vaporization). During Stage II (decomposition of hemicellulose and cellulose), blend ratio of 5:5 resulted in greater mass loss rate than ratio of 8:2 at heating rates 10-50 K/min. Dewangan, Pradhan, and Singh [40] reported that increasing LDPE ratio in binary mixtures indicates increasing degree of conversion due to synergistic effect and hence the increased mass loss rate. Likewise, the same could be deduced for the increased HDPE ratio from 5:5 to 8:2 in the binary mixtures HDPE/PKS which leads to the high mass loss rate. However, further increasing the heating rate to 100 K/min have led to apparent reduction rate of mass loss. Studies conducted by Yorgun and Yildiz [41] and Akhtar and Amin [39] have suggested that lower heating rates and longer residence time promote

399 greater conversion rate and formation of gaseous products. In this case, the high heating
400 rate and possibly shorter residence time may have resulted in the low thermal degradation
401 rate due to limited time available for secondary reactions such as tar cracking and
402 repolymerization. During Stage III (decomposition of HDPE), blend ratio of 2:8
403 demonstrated much lower maximum mass loss rate for heating rate above 20 K/min. This
404 could be the result of increased reaction time to decompose HDPE components in the
405 binary mixtures due to its high thermal stability.

406 Generally, all the three catalysts have shown evident reduction in the rate of maximum
407 degradation for the pyrolysis of PKS/HDPE mixture. Similar observations were also
408 reported by Fong et al. [22] and Majid et al. [34] with the catalytic pyrolysis of *Chlorella*
409 *vulgaris* and co-pyrolysis of *Chlorella vulgaris*/HDPE.

410

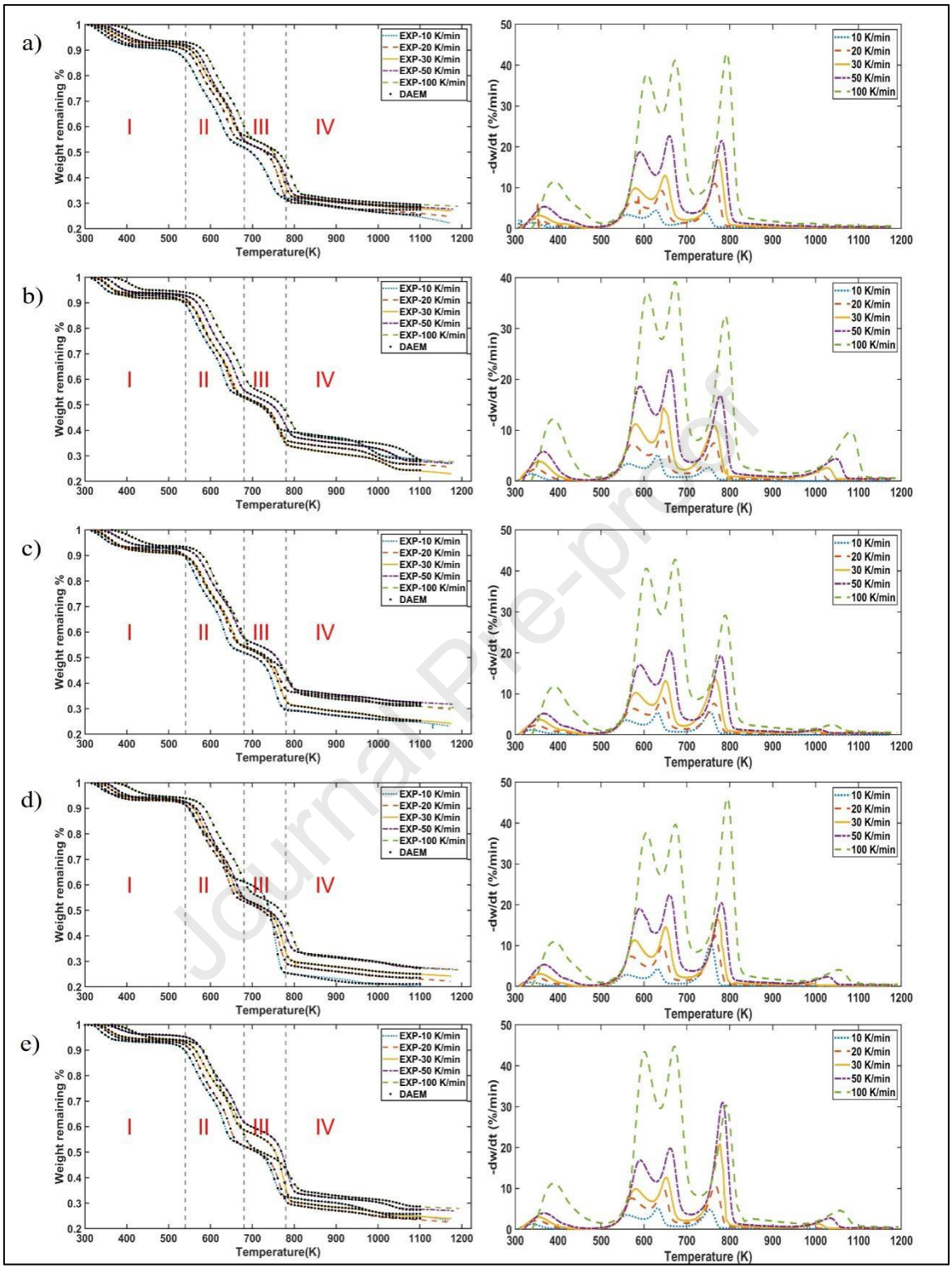

411

412 **Fig. 2.** TG and DTG curves for catalytic pyrolysis of binary mixture of PKS/HDPE in
413 different blend ratios at heating rates of 10, 20, 30, 50 and 100 K min^{-1} using different
414 catalysts (a) PKS/HDPE (2:8) using HZSM-5, (b) PKS/HDPE (2:8) using LS, (c)

PKS/HDPE (2:8) using bifunctional catalyst HZSM-5/LS, (d) PKS/HDPE (5:5) using bifunctional catalyst HZSM-5/LS, and (e) PKS/HDPE (8:2) using bifunctional catalyst HZSM-5/LS.

3.2 Kinetic Analysis

The kinetic parameters for the pyrolysis of PKS, HDPE and binary mixture of PKS and HDPE were analysed via modified DAEM and iso-conversional methods such as FWO and KAS. The binary mixtures were studied with the presence and absence of catalysts namely HZSM-5, LS and bifunctional catalysts HZSM-5/LS. The analyses were done based on the assumption of first order reactions taking place. The trend of the Arrhenius plots for iso-conversional methods at different conversions were found to be resembling closely to one another, showing a negative slope for each conversion. The accuracy of the fitting plots can be determined by the R^2 values of the Arrhenius plots, all of which are mostly approaching 1.0. The R^2 values for pyrolysis of PKS and HDPE **(see supplementary materials)**, and binary mixtures of PKS and HDPE (Table 1). The FWO method produces R^2 values of range between 0.8933 and 0.9998 while the KAS method has R^2 values in the range of 0.8763 to 0.9997. Before delving further into the kinetic discussion, the understanding the idea of E_a is of necessity whereby it refers to the minimum energy required for a reaction to take place. In most cases, it is preferable to have lower E_a as it allows a reaction to occur with a faster reaction rate. The average E_a found using the three approaches for non-catalytic PKS, HDPE and binary mixture of PKS and HDPE are 137.26-145.49 kJ mol^{-1}, 247.73-250.45 kJ mol^{-1}, 168.97-172.50 kJ mol^{-1} respectively. As for the catalytic binary mixture of PKS and HDPE in blend ratio of 2:8, the average E_a values are 149.74-152.79 kJ mol^{-1}, 115.30-120.39 kJ mol^{-1} and 124.36-129.41 kJ mol^{-1} for HZSM-5, LS and bifunctional HZSM-5/LS catalysts respectively. For binary mixture of blend ratio of 5:5 and 8:2 using bifunctional HZSM-5/LS catalysts, the average E_a values are 151.03-154.47 kJ mol^{-1} and 152.67-157.31 kJ mol^{-1} respectively.

Based on the average E_a values obtained from the three kinetic modelling methods, E_a of the pyrolysis process for each experiment was generally reduced. The reduction in E_a due to the presence of catalyst was particularly prominent for pyrolysis of binary mixture of PKS and HDPE at the same blend ratio of 2:8. Among the three types of catalysts used for this study, the LS catalyst shows great potential in reducing the E_a of the pyrolysis process of the binary mixture. This is evidenced from the decreased in average E_a value calculated using FWO, from 171.01 kJ mol^{-1} to 120.39 kJ mol^{-1}, which is a 29.6% reduction. Bifunctional HZSM-5/LS catalyst also shows significant fall in average E_a value by a percentage of 24.9%. However, the bifunctional HZSM-5/LS catalyst appears to be less effective for the binary mixture at blend ratio of 5:5 and 8:2 as the percentage reduction is around 9-10%. Likewise, HZSM-5 has also contributed rather smaller effect in lowering the E_a of the pyrolysis process of the binary mixture compared to the other catalysts used, where the activation energy was reduced by 10.7%.

Pertaining to the A value, it was found to be increasing alongside with the E_a and shows similar trend of change when the conversion factor increases from 0.1 to 0.9. The A tells the degree of collisions when a reaction takes place. It also relates to the structure of the sample whereby a loose complex will have a high factor [43]. Therefore, an increase in E_a implies slower reaction rate and consequently resulting in greater need for heat energy to achieve higher frequency of collision to allow the pyrolysis reaction to occur [44]. For both kinetic parameters, pyrolysis of PKS and binary mixture of PKS and HDPE have the maximum E_a and A attained at conversion factor of 0.7 as per shown in Fig. 3. This is regardless of the presence or absence of catalyst. As for the pyrolysis of HDPE, the kinetic parameters reach the maximum values at conversion 0.1. The average A values computed using the iso-conversional and DAEM methods for non-catalytic pyrolysis of PKS, HDPE

and binary mixture of PKS and HDPE are 6.62×10^{13}-1.03×10^{14} s^{-1}, 7.61×10^{21}-1.36×10^{28} s^{-1} and 5.78×10^{14}-3.07×10^{20} s^{-1} respectively. Catalytic pyrolysis of binary mixture of PKS and HDPE at blend ratio of 2:8 have average *A* values of 2.02×10^{13}-3.93×10^{18} s^{-1}, 2.26×10^{10}-1.33×10^{19} s^{-1} and 1.42×10^{11}-3.71×10^{14} s^{-1} respectively. For similar mixture condition but at blend ratio of 5:5 and 8:2, the average *A* values are 6.12×10^{12}-2.54×10^{31} s^{-1} and 3.08×10^{13}-7.17×10^{35} s^{-1} respectively.

The kinetic modelling results generally show rather small difference in terms of the E_a despite using different modelling methods. This can be observed from Fig. 3. However, the matrix inversion algorithm had contributed to some differences in terms of the E_a and *A* compared to the iso-conversional methods. For instance, the E_a for pyrolysis of PKS calculated using this algorithm had resulted in a much higher E_a value when compared to the iso-conversional methods as shown in Fig. 3(a). This is attributable to reactions occurring simultaneously at a particular conversion [45]. Nevertheless, the E_a values obtained for the pyrolysis of PKS and HDPE using the FWO, KAS and DAEM methods agreed well with the literature values. The E_a for pyrolysis of PKS from the available literature generally range from 40.49 to 217.04 kJ mol^{-1} [26-27,29]. However, Ma et al. [46] have reported substantially higher E_a for decomposing PKS. This is attributable to factors such as biomass species, particle size, heating rate and kinetic models applied [46]. As for the pyrolysis of HDPE, the literature values range from 207.43-473.05 kJ mol^{-1} [30-32,47].

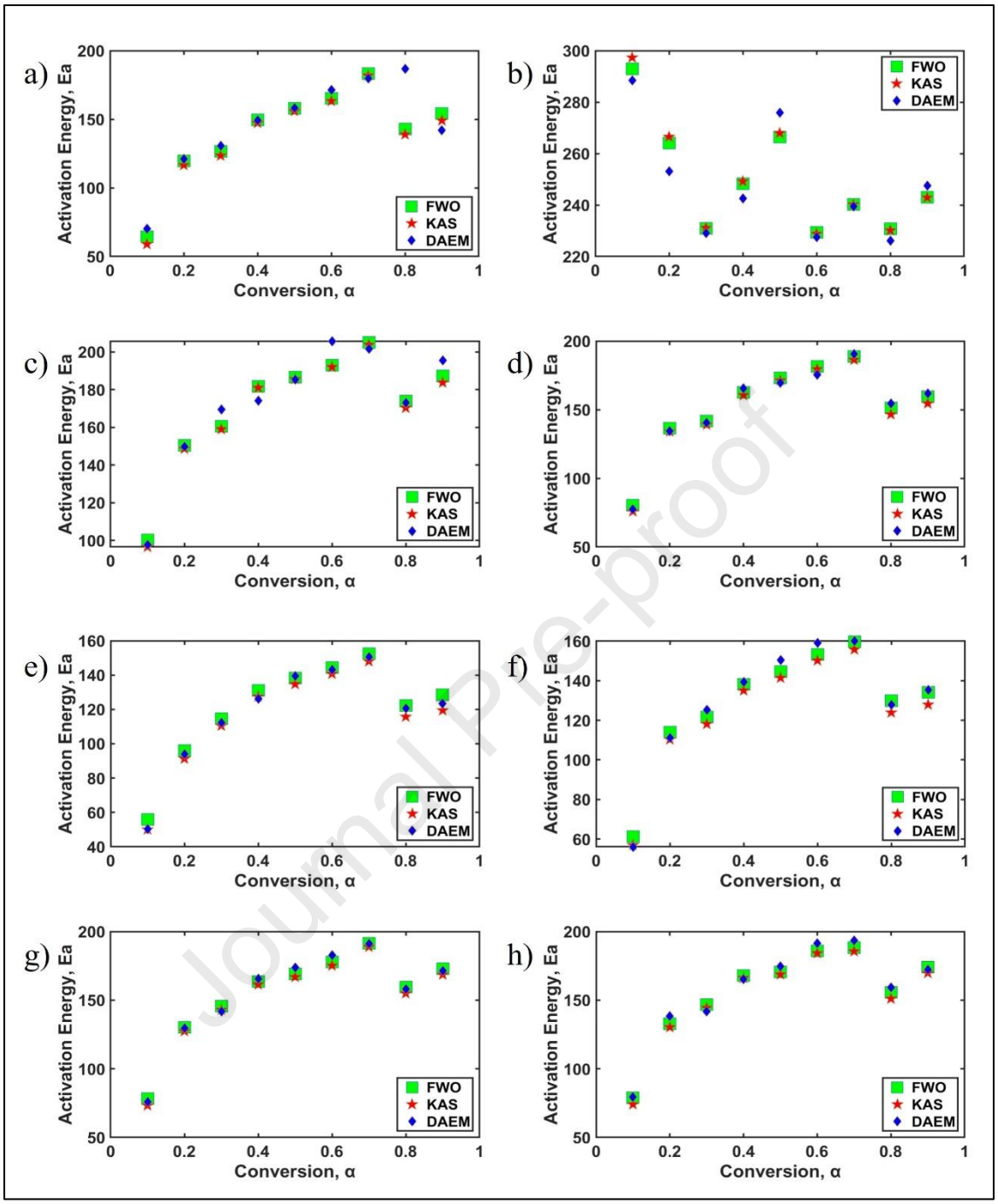

Fig. 3. Comparison of activation energies computed by FWO, KAS and modified DAEM for (a) non-catalytic pyrolysis of PKS, (b) non-catalytic pyrolysis of HDPE, (c) non-catalytic pyrolysis of binary mixture of PKS/HDPE, (d) catalytic pyrolysis of binary mixture of PKS/HDPE (2:8) using HZSM-5, (e) catalytic pyrolysis of binary mixture of PKS/HDPE (2:8) using LS, (f) catalytic pyrolysis of binary mixture of PKS/HDPE (2:8)

493 using bifunctional catalyst HZSM-5/LS, (g) catalytic pyrolysis of binary mixture of
494 PKS/HDPE (5:5) using bifunctional catalyst HZSM-5/LS, and (h) catalytic pyrolysis of
495 binary mixture of PKS/HDPE (8:2) using bifunctional catalyst HZSM-5/LS.

496 **Table 1:** Activation energy (E_a) and pre-exponential factor (A) of non-catalytic and catalytic co-pyrolysis of binary mixture of PKS and

497 HDPE at different blend ratios for each conversion factor (α), with the use of HZSM-5, LS and bifunctional HZSM-5/LS catalysts.

		Iso-conversional Methods						**Modified DAEM**	
		FWO			KAS				
	α	E_a (kJ mol^{-1})	A (s^{-1})	R^2	E_a (kJ mol^{-1})	A (s^{-1})	R^2	E_a (kJ mol^{-1})	A (s^{-1})
HDPE:PKS (2:8)	0.10	100.22	9.28×10^{8}	0.9089	96.57	2.99×10^{8}	0.8940	97.65	3.23×10^{9}
	0.20	150.40	1.74×10^{13}	0.9949	148.62	1.10×10^{13}	0.9943	149.75	7.84×10^{17}
	0.30	160.59	7.40×10^{13}	0.9745	159.01	5.02×10^{13}	0.9713	169.44	6.10×10^{19}
	0.40	181.86	1.84×10^{15}	0.9951	181.00	1.49×10^{15}	0.9946	174.22	3.84×10^{19}
	0.50	186.64	1.38×10^{15}	0.9784	185.60	1.09×10^{15}	0.9760	185.37	7.30×10^{19}
	0.60	193.05	2.14×10^{15}	0.9707	192.02	1.69×10^{15}	0.9674	205.80	2.58×10^{21}
	0.70	205.16	1.14×10^{15}	0.9712	203.83	8.69×10^{14}	0.9680	201.59	7.36×10^{15}
	0.80	174.03	1.57×10^{12}	0.9802	170.33	7.52×10^{11}	0.9771	173.10	5.60×10^{11}
	0.90	187.19	7.40×10^{12}	0.9551	183.74	3.83×10^{12}	0.9486	195.55	1.53×10^{19}
	Average	**171.01**	$\mathbf{7.34 \times 10^{14}}$	**0.9699**	**168.97**	$\mathbf{5.78 \times 10^{14}}$	**0.9657**	**172.50**	$\mathbf{3.07 \times 10^{20}}$
HDPE:PKS (2:8) - HZSM-5	0.10	80.31	2.58×10^{7}	0.9851	75.87	5.54×10^{6}	0.9813	77.33	4.53×10^{9}
	0.20	136.57	9.76×10^{11}	0.9911	134.07	5.07×10^{11}	0.9896	134.37	3.20×10^{15}
	0.30	141.60	1.49×10^{12}	0.9917	139.05	7.83×10^{11}	0.9905	140.41	3.09×10^{17}
	0.40	162.51	3.18×10^{13}	0.9653	160.58	2.01×10^{13}	0.9609	165.63	5.35×10^{17}
	0.50	173.02	9.52×10^{13}	0.9854	171.25	6.37×10^{13}	0.9836	169.51	3.42×10^{19}
	0.60	181.40	1.16×10^{14}	0.9837	179.50	7.67×10^{13}	0.9816	175.42	1.51×10^{17}
	0.70	188.84	3.29×10^{13}	0.9924	186.32	1.99×10^{13}	0.9914	190.69	2.13×10^{17}
	0.80	151.40	4.04×10^{10}	0.9939	146.54	1.45×10^{10}	0.9930	154.56	8.71×10^{12}
	0.90	159.45	9.55×10^{10}	0.9526	154.47	3.50×10^{10}	0.9442	161.87	2.90×10^{14}
	Average	**152.79**	$\mathbf{3.09 \times 10^{13}}$	**0.9823**	**149.74**	$\mathbf{2.02 \times 10^{13}}$	**0.9796**	**152.20**	$\mathbf{3.93 \times 10^{18}}$

HDPE:PKS (2:8) - LS	0.10	55.83	7.06×10^{4}	0.9789	50.06	6.86×10^{3}	0.9726	50.25	7.31×10^{8}
	0.20	95.95	1.62×10^{8}	0.9807	91.26	3.96×10^{7}	0.9761	93.92	3.50×10^{12}
	0.30	114.57	4.82×10^{9}	0.9791	110.45	1.57×10^{9}	0.9748	112.33	1.18×10^{15}
	0.40	131.12	6.48×10^{10}	0.9649	127.43	2.57×10^{10}	0.9588	126.24	1.75×10^{16}
	0.50	138.36	1.34×10^{11}	0.9836	134.69	5.53×10^{10}	0.9807	139.43	1.73×10^{18}
	0.60	144.41	2.26×10^{11}	0.9775	140.71	9.55×10^{10}	0.9737	143.26	9.86×10^{19}
	0.70	152.54	6.61×10^{10}	0.9623	147.99	2.51×10^{10}	0.9559	150.61	1.80×10^{19}
	0.80	122.34	3.38×10^{8}	0.9336	115.73	7.45×10^{7}	0.9189	120.58	1.48×10^{18}
	0.90	128.44	3.24×10^{7}	0.9386	119.42	5.28×10^{6}	0.9226	123.54	5.01×10^{6}
	Average	**120.39**	**5.51×10^{10}**	**0.9666**	**115.30**	**2.26×10^{10}**	**0.9593**	**117.79**	**1.33×10^{19}**
HDPE:PKS (2:8) - HZSM-5/LS	0.10	61.23	2.64×10^{6}	0.9769	56.89	4.25×10^{5}	0.9706	56.10	2.32×10^{8}
	0.20	113.90	8.91×10^{9}	0.9930	110.25	3.20×10^{9}	0.9916	111.12	2.25×10^{10}
	0.30	121.61	2.80×10^{10}	0.9930	118.08	1.08×10^{10}	0.9919	125.26	1.24×10^{14}
	0.40	138.20	2.81×10^{11}	0.9904	135.00	1.27×10^{11}	0.9889	139.42	1.95×10^{14}
	0.50	144.60	4.92×10^{11}	0.9865	141.40	2.29×10^{11}	0.9846	150.39	7.89×10^{14}
	0.60	153.26	1.48×10^{12}	0.9967	150.16	7.26×10^{11}	0.9962	159.04	1.60×10^{15}
	0.70	159.58	4.03×10^{11}	0.9980	155.72	1.77×10^{11}	0.9977	160.16	5.37×10^{11}
	0.80	129.84	1.42×10^{9}	0.9374	123.87	3.70×10^{8}	0.9249	127.92	6.34×10^{14}
	0.90	134.12	1.62×10^{9}	0.9857	127.87	$4.16E \times 10^{8}$	0.9828	135.25	2.64×10^{6}
	Average	**128.48**	**2.99×10^{11}**	**0.9842**	**124.36**	**1.42×10^{11}**	**0.9810**	**129.41**	**3.71×10^{14}**
HDPE:PKS (5:5) - HZSM-5/LS	0.10	78.23	6.31×10^{6}	0.9870	73.24	1.15×10^{6}	0.9832	76.00	2.84×10^{13}
	0.20	130.28	2.08×10^{11}	0.9934	127.38	9.66×10^{10}	0.9923	129.62	1.34×10^{28}
	0.30	145.47	2.18×10^{12}	0.9847	142.96	1.17×10^{12}	0.9825	141.86	2.93×10^{29}
	0.40	163.48	2.46×10^{13}	0.9771	161.37	1.51×10^{13}	0.9738	165.72	4.27×10^{29}
	0.50	169.04	2.78×10^{13}	0.9635	166.83	1.69×10^{13}	0.9585	173.62	2.47×10^{31}
	0.60	177.95	9.21×10^{12}	0.9887	175.14	5.16×10^{12}	0.9870	182.69	5.99×10^{31}
	0.70	191.45	2.74×10^{13}	0.9960	188.81	1.63×10^{13}	0.9954	191.15	1.41×10^{32}

	0.80	159.55	1.15×10^{11}	0.9847	154.93	4.46×10^{10}	0.9820	158.04	1.57×10^{30}
	0.90	172.90	6.57×10^{11}	0.9475	168.59	2.83×10^{11}	0.9392	171.54	9.11×10^{26}
	Average	**154.26**	**1.02×10^{13}**	**0.9803**	**151.03**	**6.12×10^{12}**	**0.9771**	**154.47**	**2.54×10^{31}**
HDPE:PKS (8:2) - HZSM-5/LS	0.10	78.97	6.49×10^{6}	0.9815	74.05	1.22×10^{6}	0.9773	79.32	8.41×10^{12}
	0.20	132.96	3.52×10^{11}	0.9264	130.27	1.73×10^{11}	0.9162	138.27	4.20×10^{22}
	0.30	146.74	3.00×10^{12}	0.9860	144.35	1.66×10^{12}	0.9841	141.73	4.06×10^{15}
	0.40	167.90	6.37×10^{13}	0.9629	166.14	4.23×10^{13}	0.9583	165.42	3.87×10^{18}
	0.50	170.69	4.84×10^{13}	0.9736	168.73	3.10×10^{13}	0.9704	174.53	2.95×10^{19}
	0.60	185.84	2.76×10^{14}	0.9772	184.18	1.93×10^{14}	0.9743	191.53	6.45×10^{36}
	0.70	188.31	1.56×10^{13}	0.9456	185.55	9.07×10^{12}	0.9386	193.49	3.12×10^{17}
	0.80	155.73	6.96×10^{10}	0.9501	151.03	2.62×10^{10}	0.9419	159.10	3.45×10^{12}
	0.90	174.06	5.88×10^{11}	0.9699	169.73	2.54×10^{11}	0.9651	172.43	1.76×10^{12}
	Average	**155.69**	**4.53×10^{13}**	**0.9637**	**152.67**	**3.08×10^{13}**	**0.9585**	**157.31**	**7.17×10^{35}**

498

3.3 Thermodynamic Analysis

The thermodynamic parameters for the pyrolysis of PKS, HDPE and binary mixture of PKS and HDPE under non-catalytic and catalytic conditions were calculated and tabulated in Tables 2 and 3. The ΔH represents the total energy consumed by the sample during the pyrolysis reaction which leads to the formation of volatiles and char. In this study, relatively small differences were observed between ΔH and E_a whereby the percentage differences are less than 10%, not more than 8 kJ.mol^{-1}. The minor differences suggest that the potential energy barrier between the molecules of the samples could be reduced and therefore allowing efficient formation of an activated complex [22,34,48]. Besides that, the sign of the ΔH values also indicates what type of reaction is undergoing. Referring to Tables 2 and 3, it is evident that the pyrolysis reaction in this study is of an endothermic reaction as positive values were obtained for all experiments. This entails heat being absorbed to break and form new chemical bonds. The average ΔH values calculated using FWO for non-catalytic pyrolysis of PKS, HDPE and binary mixture of PKS and HDPE are 135.17 kJ.mol^{-1}, 243.53 kJ.mol^{-1} and 165.54 kJ.mol^{-1} respectively. For catalytic pyrolysis of binary mixture of PKS and HDPE at the same blend ratio (2:8) using HZSM-5, LS and bifunctional HZSM-5/LS catalysts, the average ΔH values are 147.30 kJ.mol^{-1}, 114.74 kJ.mol^{-1} and 123.08 kJ.mol^{-1} for respectively. For similar catalytic conditions but different blend ratio of binary mixture, the average ΔH values are 148.65 kJ.mol^{-1} and 150.12 kJ.mol^{-1} for 5:5 and 8:2 blend ratios respectively.

The ΔG is the total energy increased in a system where formation of activated complex takes place. Low ΔG values indicates that formation of products is feasible even with low energy supply [34]. The ΔG values for the pyrolysis of PKS and HDPE are 157.95 kJ.mol^{-1} and 182.93 kJ.mol^{-1}. In the case of non-catalytic and catalytic pyrolysis of binary mixture

of PKS and HDPE using HZSM-5, the ΔG values are 165.13 kJ.mol^{-1} and 165.95 kJ.mol^{-1}. The use of bifunctional HZSM-5/LS and LS catalyst in place of HZSM-5 for the same binary mixture of blend ratio 2:8 have ΔG values of 163.39 kJ.mol^{-1} and 171.43 kJ.mol^{-1}, respectively. As for the catalytic pyrolysis of the binary mixture at blend ratios 5:5 and 8:2 using the three different catalysts, the ΔG values are 169.69 kJ.mol^{-1} and 168.47 kJ.mol^{-1}, respectively. It can be deduced from the ΔG values that the pyrolysis of PKS, HDPE and binary mixture of PKS and HDPE are potential biofuel production feedstock.

Meanwhile, ΔS reflects how near a system approaching thermodynamic equilibrium. Generally, a high ΔS may be anticipated as it signifies high reactivity and requires short amount of time to produce an activated complex [49]. It is noticed that the average ΔS values for PKS and the binary mixtures of PKS and HDPE in this study are negative, while HDPE has positive average ΔS values. In simpler terms, if the entropy value is less than zero, the reaction would be reactant-favoured while the opposite would be product-favoured. The negative average ΔS values implies thermodynamic equilibrium was achieved and that the formation of activation complex was highly organized. Meanwhile, high entropy values shown by HDPE suggests high reactivity due to highly disordered particles whereby relatively shorter reaction time allows the formation of activated complex [22,50].

In summary, ΔH is linked to the E_a whereby the small percentage difference between the two parameters in the present study indicates that there will be low potential energy barrier and thus promoting the production of activated complex. Additionally, positive ΔH values in this study further ascertains that the pyrolysis process is an endothermic reaction. Positive ΔG values also implies that the process is endothermic and non-spontaneous. On the other hand, the thermal equilibrium state achieved by the feedstock

except HDPE is confirmed by the negative ΔS values which also means high degree of order was attained in the activated complex formation.

549 **Table 2:** Enthalpy change, Gibb's free energy and entropy change of pyrolysis of PKS and HDPE at each conversion factor (α).

		FWO			KAS		
	α	ΔH (kJ/mol)	ΔG (kJ/mol)	ΔS (J/mol)	ΔH (kJ/mol)	ΔG (kJ/mol)	ΔS (J/mol)
PKS	0.10	59.89	139.18	-149.97	54.56	142.76	-166.83
	0.20	115.01	146.33	-55.26	111.87	147.32	-62.56
	0.30	121.73	148.41	-45.79	118.62	149.33	-52.70
	0.40	144.48	151.02	-10.90	142.28	151.54	-15.43
	0.50	152.89	155.83	-4.72	150.78	156.33	-8.89
	0.60	159.99	159.28	1.10	157.93	159.76	-2.84
	0.70	177.76	161.31	25.03	176.36	161.63	22.42
	0.80	137.22	167.16	-43.87	133.26	168.40	-51.48
	0.90	147.56	193.03	-57.59	142.50	194.82	-66.28
	Average	**135.17**	**157.95**	**-38.00**	**132.02**	**159.10**	**-44.95**
HDPE	0.10	287.54	171.19	177.36	291.85	171.97	182.75
	0.20	258.48	176.18	120.23	260.82	176.52	123.14
	0.30	225.07	182.52	59.66	225.16	182.71	59.52
	0.40	242.26	184.28	79.55	243.12	184.47	80.47
	0.50	260.24	184.76	102.11	261.81	185.02	103.89
	0.60	223.09	186.40	49.06	222.59	186.62	48.09
	0.70	233.99	186.84	62.31	233.90	187.05	61.92
	0.80	224.47	187.40	48.48	223.77	187.64	47.25
	0.90	236.66	186.81	64.56	236.45	187.03	64.01
	Average	**243.53**	**182.93**	**84.81**	**244.39**	**183.23**	**85.67**

550

551 **Table 3:** Enthalpy change, Gibb's free energy and entropy change of non-catalytic and catalytic co-pyrolysis of binary mixture of PKS and HDPE

552 at different blend ratios for each conversion factor (α), with the use of HZSM-5, LS and bifunctional HZSM-5/LS catalysts.

		FWO			KAS		
	α	Δ*H* (kJ/mol)	Δ*G* (kJ/mol)	Δ*S* (J/mol)	Δ*H* (kJ/mol)	Δ*G* (kJ/mol)	Δ*S* (J/mol)
HDPE:PKS (2:8)	0.10	95.73	142.41	-86.49	92.09	143.84	-95.90
	0.20	145.60	148.63	-5.26	143.83	149.03	-9.02
	0.30	155.63	151.74	6.51	154.04	152.09	3.28
	0.40	176.69	156.26	32.87	175.83	156.49	31.12
	0.50	181.26	161.70	30.18	180.21	161.96	28.17
	0.60	187.51	165.14	33.56	186.48	165.40	31.63
	0.70	199.13	179.09	27.65	197.80	179.41	25.37
	0.80	167.66	188.77	-27.57	163.97	189.77	-33.71
	0.90	180.63	192.43	-14.96	177.19	193.29	-20.42
	Average	**165.54**	**165.13**	**-0.39**	**163.49**	**165.70**	**-4.39**
HDPE:PKS (2:8) - HZSM-5	0.10	76.01	135.84	-115.90	71.58	138.00	-128.70
	0.20	131.79	148.58	-29.17	129.29	149.21	-34.61
	0.30	136.64	152.12	-25.94	134.09	152.78	-31.31
	0.40	157.31	157.88	-0.91	155.37	158.32	-4.70
	0.50	167.62	162.49	7.90	165.85	162.89	4.56
	0.60	175.73	169.52	9.11	173.83	169.95	5.70
	0.70	182.66	184.19	-2.06	180.14	184.77	-6.24
	0.80	145.02	189.57	-58.05	140.16	191.27	-66.58
	0.90	152.87	193.32	-51.14	147.90	194.94	-59.49
	Average	**147.30**	**165.95**	**-29.57**	**144.25**	**166.90**	**-35.71**
HDPE:PKS (2:8) - LS	0.10	51.45	138.44	-165.14	45.68	142.89	-184.52
	0.20	91.14	150.00	-101.58	86.44	152.09	-113.31

	0.30	109.56	153.97	-73.71	105.44	155.47	-83.03
	0.40	125.90	158.81	-52.44	122.21	159.95	-60.14
	0.50	132.95	163.34	-46.71	129.28	164.45	-54.06
	0.60	138.82	167.47	-42.63	135.12	168.57	-49.78
	0.70	146.30	186.59	-53.75	141.76	188.08	-61.80
	0.80	115.89	191.82	-97.89	109.28	194.97	-110.48
	0.90	120.62	232.42	-118.99	111.61	237.58	-134.07
	Average	**114.74**	**171.43**	**-83.65**	**109.65**	**173.78**	**-94.58**
HDPE:PKS (2:8) - HZSM-5/LS	0.10	57.47	117.96	-133.75	53.13	120.49	-148.95
	0.20	109.13	148.23	-68.18	105.49	149.47	-76.71
	0.30	116.67	151.73	-58.97	113.13	152.90	-66.87
	0.40	133.00	158.16	-40.22	129.80	159.08	-46.82
	0.50	139.22	162.44	-35.85	136.02	163.35	-42.21
	0.60	147.73	165.66	-26.94	144.62	166.49	-32.85
	0.70	153.50	181.68	-38.52	149.64	182.81	-45.35
	0.80	123.48	189.20	-85.83	117.50	191.81	-97.04
	0.90	127.48	195.42	-85.10	121.23	198.20	-96.42
	Average	**123.08**	**163.39**	**-63.71**	**118.95**	**164.96**	**-72.58**
HDPE:PKS (5:5) - HZSM-5/LS	0.10	73.72	143.16	-128.03	68.73	145.84	-142.17
	0.20	125.45	149.86	-42.08	122.56	150.66	-48.46
	0.30	140.44	154.30	-22.90	137.93	154.92	-28.08
	0.40	158.20	160.20	-3.15	156.10	160.67	-7.21
	0.50	163.56	165.18	-2.46	161.35	165.68	-6.58
	0.60	171.93	180.92	-12.41	169.12	181.59	-17.23
	0.70	185.16	187.98	-3.73	182.51	188.59	-8.03
	0.80	153.11	191.40	-49.42	148.49	192.88	-57.30
	0.90	166.29	194.23	-35.15	161.98	195.48	-42.14
	Average	**148.65**	**169.69**	**-33.26**	**145.42**	**170.70**	**-39.69**
HDPE:PKS (8:2) - HZSM-5/LS	0.10	74.43	144.30	-127.86	69.51	146.98	-141.78

0.20	128.13	150.04	-37.72	125.44	150.78	-43.63
0.30	141.72	153.93	-20.23	139.33	154.52	-25.16
0.40	162.64	159.61	4.78	160.88	160.01	1.38
0.50	165.25	163.80	2.21	163.29	164.25	-1.47
0.60	180.18	169.05	16.36	178.52	169.42	13.38
0.70	182.01	188.39	-8.41	179.25	189.05	-12.93
0.80	149.31	190.65	-53.56	144.61	192.23	-61.69
0.90	167.39	196.43	-36.16	163.05	197.71	-43.15
Average	**150.12**	**168.47**	**-28.95**	**147.10**	**169.44**	**-35.01**

553

554

555 **4.0 Conclusion**

556 Thermal degradation behaviour, kinetic and thermodynamic studies on the catalytic co-
557 pyrolysis of PKS and HDPE mixtures were investigated with the presence of different catalysts
558 (zeolite HZSM-5, LS and bifunctional HZSM-5/LS). It is found that the presence of the LS
559 catalyst in the co-pyrolysis PKS/HDPE mixtures shown the best performance when compared
560 with the other two catalysts. A reduction of 30% was successfully achieved in the activation
561 energy and enthalpy energy change for these mixtures using FWO method. It is found that the
562 values for both ΔH and ΔG for the catalytic co-pyrolysis of PKS/HDPE mixtures are in positive
563 values which shows the process is in endothermic reaction and possess non-spontaneous nature.
564 Furthermore, obvious changes had been observed in the ΔH and ΔS with the conversion factor.
565 The outcomes of the present study would be beneficial in providing the necessary information
566 needed for upscaling, design and optimisation for this process. Future recommendations to be
567 suggested in this study are as follows: a) Different types of palm oil residues and plastic wastes
568 to be incorporated in the pyrolysis process for thermogravimetric analysis (TGA) studies, b)
569 Various thermochemical conversion such as gasification, hydrothermal, valorisation to be
570 introduced using the PKS and HDPE as feedstock for kinetic and thermodynamic analyses, and
571 (c) Incorporate machine learning approach for the determination of the kinetic and
572 thermodynamic parameters in the catalytic co-pyrolysis of PKS/HDPE mixtures.

573 **Acknowledgements**

574 The authors would like to thank Curtin University Malaysia and biomass processing laboratory,
575 Centre of Biofuel and Biochemical (CBBR) of Universiti Teknologi PETRONAS (UTP) for
576 the technical support. And also, this work is also supported by JASTIP-Net 2022 Collaborative
577 Research, Japan on the project 'Techno-economics/Environmental/Societal/Governmental

(TESG) evaluation of thermochemical conversion of oil palm residues to alternative energies for ASEAN region'.

References

[1] Yildiz L. Fossil Fuels. Compr. Energy Syst., vol. 1–5, Elsevier Inc.; 2018, p. 521–67. https://doi.org/10.1016/B978-0-12-809597-3.00111-5.

[2] Liew RK, Nam WL, Chong MY, Phang XY, Su MH, Yek PNY, et al. Oil palm waste: An abundant and promising feedstock for microwave pyrolysis conversion into good quality biochar with potential multi-applications. Process Safety Environ Prot 2018;115:57–69. https://doi.org/10.1016/j.psep.2017.10.005.

[3] Zhao L, Cao X, Mašek O, Zimmerman A. Heterogeneity of biochar properties as a function of feedstock sources and production temperatures. J Hazard Mater 2013;256–257:1–9. https://doi.org/10.1016/j.jhazmat.2013.04.015.

[4] Idris R, Chong WWF, Ali A, Idris S, Hasan MF, Ani FN, et al. Phenol-rich bio-oil derivation via microwave-induced fast pyrolysis of oil palm empty fruit bunch with activated carbon. Environ Technol Innov 2021;21:101291. https://doi.org/10.1016/j.eti.2020.101291.

[5] Shafaghat H, Lee HW, Tsang YF, Oh D, Jae J, Jung SC, et al. In-situ and ex-situ catalytic pyrolysis/co-pyrolysis of empty fruit bunches using mesostructured aluminosilicate catalysts. Chem Eng J 2019;366:330–8. https://doi.org/10.1016/j.cej.2019.02.055.

[6] Supian MAF, Amin KNM, Jamari SS, Mohamad S. Production of cellulose nanofiber (CNF) from empty fruit bunch (EFB) via mechanical method. J Environ Chem Eng 2020;8:103024. https://doi.org/10.1016/j.jece.2019.103024.

[7] Geyer R, Jambeck JR, Law KL. Production, use, and fate of all plastics ever made, Sci Adv 2017,3, e1700782.

[8] Lebreton L, Andrady A. Future scenarios of global plastic waste generation and disposal, Palgrave Communications 2019,5,1-11.

603 [9] Qureshi MS, Oasmaa A, Pihkola H, Deviatkin I, Tenhunen A, Mannila J, et al. Pyrolysis of
604 plastic waste: Opportunities and challenges. J Anal Appl Pyrolysis 2020;152:104804.
605 https://doi.org/https://doi.org/10.1016/j.jaap.2020.104804.

606 [10] Nsaful F, Görgens JF, Knoetze JH. Comparison of combustion and pyrolysis for energy
607 generation in a sugarcane mill. Energy Convers Manag 2013;74:524–34.
608 https://doi.org/10.1016/j.enconman.2013.07.024.

609 [11] KeTTHA. National Renewable Energy Policy and Action Plan. 2009.

610 [12] Economic Planning Unit. Tenth Malaysia Plan. Putrajaya: 2011.

611 [13] Hassan H, Lim JK, Hameed BH. Recent progress on biomass co-pyrolysis conversion into high-
612 quality bio-oil. Bioresour Technol 2016;221:645–55.
613 https://doi.org/10.1016/j.biortech.2016.09.026.

614 [14] Chen W, Shi S, Zhang J, Chen M, Zhou X. Co-pyrolysis of waste newspaper with high-density
615 polyethylene: Synergistic effect and oil characterization. Energy Convers Manag 2016;112:41–
616 8. https://doi.org/10.1016/j.enconman.2016.01.005.

617 [15] Hassan H, Lim JK, Hameed BH. Catalytic co-pyrolysis of sugarcane bagasse and waste high-
618 density polyethylene over faujasite-type zeolite. Bioresour Technol 2019;284:406–14.
619 https://doi.org/10.1016/j.biortech.2019.03.137.

620 [16] Ma Z, Troussard E, Van Bokhoven JA. Controlling the selectivity to chemicals from lignin via
621 catalytic fast pyrolysis. Appl Catal A Gen 2012;423–424:130–6.
622 https://doi.org/10.1016/j.apcata.2012.02.027.

623 [17] Tan S, Zhang Z, Sun J, Wang Q. Recent progress of catalytic pyrolysis of biomass by HZSM-5.
624 Cuihua Xuebao/Chinese J Catal 2013;34:641–50. https://doi.org/10.1016/s1872-
625 2067(12)60531-2.

626 [18] Yap TL, Loy ACM, Chin BLF, Lim JY, Alhamzi H, Chai YH, Yiin CL, Cheah KW, Wee MXJ,
627 Lam MK, Jawad ZA, Yusup S, Lock SSM. Synergistic effects of catalytic co-pyrolysis Chlorella

vulgaris and polyethylene mixtures using artificial neuron network: Thermodynamic and empirical kinetic analyses. J Environ Chem Technol 2022,10:107391. https://doi.org/10.1016/j.jece.2022.107391.

[19] Loy ACM, Yusup S, Chin BLF, Gan DKW, Shahbaz M, Acda MN, Unrean P, Rianawati E. Comparative study of in-situ catalytic pyrolysis of rice husk for syngas production: Kinetics modelling and product gas analysis. J Clean Prod 2018;197:1231-43. https://doi.org/10.1016/j.jclepro.2018.06.245.

[20] Gan, KWD, Loy ACM, Chin BLF, Yusup S, Unrean P, Rianawati E, Acda MN. Kinetics and thermodynamic analysis in one-pot pyrolysis of rice hull using renewable calcium oxide based catalysts. Bioresour Technol 2018;265:180-90. https://doi.org/10.1016/j.biortech.2018.06.003.

[21] Yang H, Ji G, Clough PT, Xu X, Zhao M. Kinetics of catalytic biomass pyrolysis using Ni-based functional materials. Fuel Process Technol 2019;195:106145. https://doi.org/10.1016/j.fuproc.2019.106145.

[22] Fong MJB, Loy ACM, Chin BLF, Lam MK, Yusup S, Jawad ZA. Catalytic pyrolysis of Chlorella vulgaris: Kinetic and thermodynamic analysis. Bioresour Technol 2019;289:121689. https://doi.org/10.1016/j.biortech.2019.121689.

[23] Kumar AN, Chin BLF, Chee ALK. Kinetic analysis for catalytic co-pyrolysis of palm kernel shell and plastic waste mixtures with bifunctional HZSM-5 and mussel shell catalyst. IOP Conf Series: Mat Sci Eng 2022;1257:012016. https://doi.org/10.1088/1757-899X/1257/1/012016.

[24] Bong JT, Loy ACM, Chin BLF, Lam MK, Tang DKH, Lim HY, Chai YH, Yusup S. Artificial neural network approach for co-pyrolysis of Chlorella vulgaris and peanut shell binary mixtures using microalgae ash catalyst. Energy 2020;207:118289. https://doi.org/10.1016/j.energy.2020.118289.

[25] Soon VSY, Chin BLF, Lim ACR. Kinetic study on pyrolysis of oil palm frond. IOP Conf Series: Mat Sci Eng 2016;121:012004. https://doi.org/ 10.1088/1757-899X/121/1/012004.

[26] Surahmanto F, Saptoadi H, Sulistyo H, Rohmat TA. Investigation of the slow pyrolysis kinetics of oil palm solid waste by the distributed activation energy model. Biofuels 2017;11:663–70. https://doi.org/10.1080/17597269.2017.1387750.

[27] Salema AA, Ting RMW, Shang YK. Pyrolysis of blend (oil palm biomass and sawdust) biomass using TG-MS. Bioresour Technol 2019;274:439–46. https://doi.org/10.1016/j.biortech.2018.12.014.

[28] Surahmanto F, Saptoadi H. Investigation of the pyrolysis characteristics and kinetics of oil-palm solid waste by using Coats – Redfern method 2019. https://doi.org/10.1177/0144598719877759.

[29] Patrick DO, Suzana Y, Osman NB, Zabiri H, Uemura Y, Shahbaz M. Thermogravimetric Kinetics of Catalytic and Non-Catalytic Pyrolytic Conversion of Palm Kernel Shell with Acid-Treated Coal Bottom Ash 2020;13:452-62. https://doi.org/10.1007/s12155-020-10101-2.

[30] Aboulkas A, El harfi K, El bouadili A, Nadifiyine M, Benchanaa M, Mokhlisse A. Pyrolysis kinetics of olive residue/plastic mixtures by non-isothermal thermogravimetry. Fuel Process Technol 2009;90:722–8. https://doi.org/10.1016/j.fuproc.2009.01.016.

[31] Rotliwala YC, Parikh PA. Thermal degradation of rice-bran with high density polyethylene: A kinetic study. Korean J Chem Eng 2011;28:788–92. https://doi.org/10.1007/s11814-010-0414-1.

[32] Chin BLF, Yusup S, Al Shoaibi A, Kannan P, Srinivasakannan C, Sulaiman SA. Kinetic studies of co-pyrolysis of rubber seed shell with high density polyethylene. Energy Convers Manag 2014;87:746–53. https://doi.org/10.1016/j.enconman.2014.07.043.

[33] Ng QH, Chin BLF, Yusup S, Loy ACM, Chong KYY. Modeling of the co-pyrolysis of rubber residual and HDPE waste using the distributed activation energy model (DAEM). Appl Therm Eng 2018;138:336–45. https://doi.org/10.1016/j.applthermaleng.2018.04.069.

[34] Majid M, Lai B, Chin F, Abbas Z, Ho Y. Bioresource Technology Particle swarm optimization and global sensitivity analysis for catalytic co-pyrolysis of Chlorella vulgaris and plastic waste

678 mixtures. Bioresour Technol 2021;329:124874. https://doi.org/10.1016/j.biortech.2021.124874.

679 [35] Liew JX, Loy ACM, Chin BLF, AlNouss A, Shahbaz M, Al-Ansari T, Govindan R, Chai YH.
680 Syngergistic effects of catalyic co-pyrolysis of corn cob and HDPE waste mixtures using weigh
681 average global process model. Renew Energy 2021;170:948-63.
682 https://doi.org/10.1016/j.renene.2021.02.053

683 [36] Sogancioglu M, Yel E, Ahmetli G. Pyrolysis of waste high density polyethylene (HDPE) and
684 low density polyethylene (LDPE) plastics and production of epoxy composites with their
685 pyrolysis chars. J Clean Prod 2017;165:369–81.
686 https://doi.org/https://doi.org/10.1016/j.jclepro.2017.07.157.

687 [37] Carlson TR, Jae J, Lin YC, Tompsett GA, Huber GW. Catalytic fast pyrolysis of glucose with
688 HZSM-5: The combined homogeneous and heterogeneous reactions. J Catal 2010;270:110–24.
689 https://doi.org/10.1016/j.jcat.2009.12.013.

690 [38] Sebestyén Z, Barta-Rajnai E, Bozi J, Blazsó M, Jakab E, Miskolczi N, et al. Thermo-catalytic
691 pyrolysis of biomass and plastic mixtures using HZSM-5. Appl Energy 2017;207:114–22.
692 https://doi.org/10.1016/j.apenergy.2017.06.032.

693 [39] Chen X, Li S, Liu Z, Chen Y, Yang H, Wang X, et al. Pyrolysis characteristics of lignocellulosic
694 biomass components in the presence of CaO. Bioresour Technol 2019;287:121493.
695 https://doi.org/10.1016/j.biortech.2019.121493.

696 [40] Dewangan A, Pradhan D, Singh RK. Co-pyrolysis of sugarcane bagasse and low-density
697 polyethylene: Influence of plastic on pyrolysis product yield. Fuel 2016;185:508–16.
698 https://doi.org/10.1016/j.fuel.2016.08.011.

699 [41] Yorgun S, Yildiz D. Slow pyrolysis of paulownia wood: Effects of pyrolysis parameters on
700 product yields and bio-oil characterization. J Anal Appl Pyrolysis 2015;114:68–78.
701 https://doi.org/10.1016/j.jaap.2015.05.003.

702 [42] Akhtar J, Saidina Amin N. A review on operating parameters for optimum liquid oil yield in

biomass pyrolysis. Renew Sustain Energy Rev 2012;16:5101–9. https://doi.org/10.1016/j.rser.2012.05.033.

[43] Chong YY, Thangalazhy-Gopakumar S, Gan S, Ng HK, Lee LY, Adhikari S. Kinetics and Mechanisms for Copyrolysis of Palm Empty Fruit Bunch Fiber (EFBF) with Palm Oil Mill Effluent (POME) Sludge. Energy and Fuels 2017;31:8217–27. https://doi.org/10.1021/acs.energyfuels.7b00877.

[44] Zhang X, Han Y, Li Y, Sun Y. Effect of Heating Rate on Pyrolysis Behavior and Kinetic Characteristics of Siderite. Minerals 2017;7. https://doi.org/10.3390/min7110211.

[45] Scott SA, Dennis JS, Davidson JF, Hayhurst AN. An algorithm for determining the kinetics of devolatilisation of complex solid fuels from thermogravimetric experiments. Chem Eng Sci 2006;61:2339–48. https://doi.org/10.1016/j.ces.2005.11.002.

[46] Ma Z, Chen D, Gu J, Bao B, Zhang Q. Determination of pyrolysis characteristics and kinetics of palm kernel shell using TGA-FTIR and model-free integral methods. Energy Convers Manag 2015;89:251–9. https://doi.org/10.1016/j.enconman.2014.09.074.

[47] Kumar S, Singh RK. Pyrolysis kinetics of waste high-density polyethylene using thermogravimetric analysis. Int J ChemTech Res 2014;6:131–7.

[48] Ahmad M, Mehmood M, Taqvi S, Elkamel A, Liu C-G, Xu J, et al. Pyrolysis, kinetics analysis, thermodynamics parameters and reaction mechanism of Typha latifolia to evaluate its bioenergy potential. Bioresour Technol 2017;245:491–501. https://doi.org/10.1016/j.biortech.2017.08.162.

[49] Kaur R, Gera P, Jha MK, Bhaskar T. Pyrolysis kinetics and thermodynamic parameters of castor (Ricinus communis) residue using thermogravimetric analysis. Bioresour Technol 2018;250:422–8. https://doi.org/10.1016/j.biortech.2017.11.077.

[50] Rashid T, Sher F, Khan AS, Khalid U, Rasheed T, Iqbal HMN, et al. Effect of protic ionic liquid treatment on the pyrolysis products of lignin extracted from oil palm biomass. Fuel 2021;291:120133. https://doi.org/https://doi.org/10.1016/j.fuel.2021.120133.

Highlights

- Catalytic co-pyrolysis of PKS/HDPE mixtures were investigated.
- LS shows the better catalytic performance compared to HZSM-5 and HZSM-5/LS.
- Kinetic obtained via three models: FWO, KAS and modified DAEM.
- ΔG, ΔH, and ΔS obtained in 115-166, 163-174 kJ.mol^{-1}, and 0.39-95 J.mol^{-1}.

Declaration of interests

☒ The authors declare that they have no known competing financial interests or personal relationships that could have appeared to influence the work reported in this paper.

☐The authors declare the following financial interests/personal relationships which may be considered as potential competing interests: